

Effect of Pressure and Excitation Power on Up-conversion Assisted White Light Emission in Yttrium Oxide and Silicate Nanophosphors

Gonul Eryurek^{*}, Murat Erdem^{**} and Gokhan Bilir^{***}

^{*}Department of Physics Engineering, Istanbul Technical University, Istanbul, TURKEY, gozenl@itu.edu.tr

^{**}Department of Physics, Marmara University, Istanbul, TURKEY, merdem@marmara.edu.tr

^{***}Department of Physics, Kafkas University, Kars, TURKEY, bilir@bc.edu

ABSTRACT

The production of warm artificial white light (WL) become a big challenge of engineers and scientists after the revolutionary introduction of incandescent lamp by Thomas Edison. Although several strategies have been developed in past, none of them was able to reach color quality of incandescent lamp because all these technologies suffer from low Color Rendering Indexes (CRI) and/or high Correlated Color Temperatures (CCT) which are not suitable for human perception. Recently, we were able to produce white light emission from un-doped and REIs doped Yttrium Oxide and Silicates with color quality parameters comparable with those of an incandescent lamp induced by infrared laser diode excitation. The characteristics of the white light emission both from yttrium oxide and silicate and the physical parameters that affect the white light emission were determined. A detailed comparison of the white light emission from yttrium oxide and yttrium silicate were made. The role of the type and the amount of the dopant ions on the production of the white light emission were determined.

Keywords: White light, nanophosphor, XRD, absorption, emission

1 INTRODUCTION

Synthesis, structural and optical characterization of new and suitable materials are very important in photonics technology due to the increasing materials requirement as a result of the fast developments in this field. Phosphor materials doped with different +3 valence rare earth ions (REI) such as glasses, crystals, nanopowders, quantum dots (QD) etc. are candidates to meet these requirements in photonics technology. These materials have attracted more interest due to their potential applications to optoelectronics and photonics [1-4]. In particular, they have many application areas such as displays, florescent lamps, light emitting diodes and bio-sensing. Some phosphor materials converted infrared light to visible radiation, and are known as "optical transducers" [5].

In particular, among these materials, cubic Y_2O_3 (yttria) crystals with controllable sizes and morphology are

worthy of investigation due to their excellent properties, such as stability, high thermal conductivity, high corrosion

resistance, wide spectral range optical transparency (0.2 – 8 μm) and a high refractive index (~ 1.8). Also, these hosts are considered to be the best host materials for REIs due to some similarities of Y^{3+} with the REIs such as chemical properties and ionic radius. Yttria is a sesquioxide with a higher melting point ($\sim 2410^\circ\text{C}$) and a phonon energies of about $\sim 430 - 550 \text{ cm}^{-1}$ [7, 8].

The $\text{SiO}_2\text{-Y}_2\text{O}_3$ ($Y_2\text{SiO}_5$ and $Y_2\text{Si}_2\text{O}_7$) systems exhibit interesting thermal and luminescence properties that have led to applications in optical memory devices, solid-state laser systems, and phosphors [4]. The host lattice $Y_2\text{Si}_2\text{O}_7$ shows high thermal, and chemical stability [5]; it has been shown that the structural phases due to its complex high temperature polymorphism are in the γ , z , α , β , γ , and δ forms [6]. $\gamma\text{-Y}_2\text{Si}_2\text{O}_7$ is a high temperature phase among the six polymorphs of yttrium disilicate crystallizes into a monoclinic structure with a $P2_{1/c}$ space group and assigns unique crystallographic site to the Y^{3+} ions both with six coordination number [7]. However, the main challenge is the represented by preparation of this system as a single-phase material.

2 EXPERIMENTAL

2.1 Materials Preparation

2.1.1 Synthesizes of Y_2O_3 nanocrystals:

Nanosized Y_2O_3 samples were prepared by thermal decomposition of yttrium-neodymium alginate. Yttrium nitrate hexahydrate $Y(\text{NO}_3)_3 \cdot 6\text{H}_2\text{O}$ and low-viscosity (250 cps of 2% solution) alginic acid sodium salt of an analytic grade purchased from the Sigma Aldrich Company.

The yttrium-alginate beads were prepared by thermal decomposition method according to the prescription given in the literature [6]. 0,2M 100ml yttrium nitrate solution were prepared by dissolving the appropriate amount of the yttrium nitrate in ultra pure water. Also 50ml alginate

solution was prepared by dissolving an appropriate amount of the sodium alginate salt in the ultra pure water under magnetic stirring. Alginate is a biopolymer which is extracted from three species of brown algae. It is a linear heteropolysaccharide composed of D-mannuronic acid and L-guluronic acid. Gelation of alginate is possible by the interaction of the carboxylate group with divalent ions and the formation of beads can be achieved by dropwise addition of sodium alginate into divalent solution by using a syringe with a needle or pipette [7,8]. The formation of the yttrium-alginate beads was achieved by the dropwise addition of the sodium alginate solution into yttrium-neodymium salts solution by using a syringe.

The prepared beads were kept in their gelling medium for 30 minutes under gentle stirring; then they were removed from their gelling medium, placed in a porcelain crucible and heated to different temperatures ranging from 350 to 500°C for 24h with a heating rate of 10 °C/min in an electric furnace in air medium. Some of the products obtained were annealed at 1400°C.

2.1.2. Synthesizes of $Y_2Si_2O_7$ nanocrystals:

Nanocrystalline γ - $Y_2Si_2O_7$ powders were synthesized by using the sol-gel method. Precursors with the purity of 99.9% Tetraethyl orthosilicate TEOS, $(Si(OC_2H_5)_4)$, and 99.9% yttrium nitrate hexahydrate $(Y(NO_3)_6 \cdot 6H_2O)$ were used to obtain nanopowders. The SiO_2 and Y_2O_3 mole % ratio was set at 7.0. Yttrium nitrate and TEOS were separately dissolved in double distilled water and ethanol. The yttrium nitrate salt solution was kept at 70 °C under acidic conditions (1 N HNO_3) for 45 min and then left for cooling at room temperature. After the TEOS solution was added to the solution and stirred for 2.5 h, the mixed solution was placed into circular petri dishes for three weeks to obtain a gel at room temperature. After gelation process, the transparent glass sample was obtained. The glass sample was then heat-treated at 1170 °C for 12 h to produce nanocrystalline $Y_2Si_2O_7$ [9, 10].

2.2 Structural Characterization and Spectroscopic Measurements

X-ray diffraction (XRD) patterns of nanocrystalline powders were collected by Bruker AXS D8 diffractometer for a step size of $0.01^\circ/2\theta$, between 20 and 90° ; using $CuK\alpha$ ($\lambda=1.54184 \text{ \AA}$) monochromatic radiation, operating at $I=10 \text{ mA}$, $V=30 \text{ kV}$. The average particle sizes of the powders were estimated using the Scherrer equation [11].

$$L = \frac{K\lambda}{\beta \cos \theta} \quad (1)$$

where L is the average size of the ordered (crystalline) domains, K is a dimensionless shape factor that 0.89 for spherical particles ($0.89 < K < 1$), λ is the X-ray

wavelength, β is the width of the peak at half maximum (FWHM) intensity of specific phase in radians, and θ is the center angle of the considered Bragg reflection.

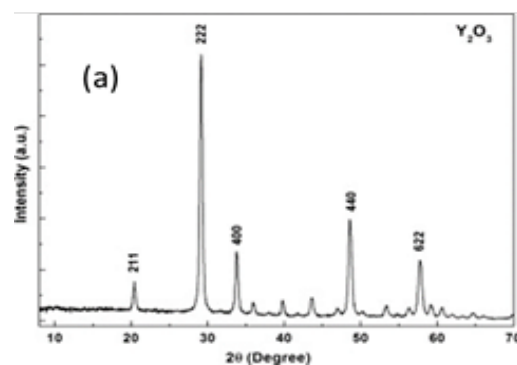
As a further confirmation of the average particle size, SEM images of the samples were obtained by a JEOL 6335F model scanning electron microscope.

The continuous emission WL spectra were produced by pumping the samples with the output of a Laser Drive Inc. Model LDI-820 laser diode operating at 803.5 nm with the maximum output power of 3 W or of a similar diode operating at 975 nm with the maximum output of 10 W. The signal was directed toward the entrance slit of a 1 m McPherson Model 2051 monochromator and chopped at a frequency of 250 Hz before entering the slit. The monochromator provided a resolution 0.8 \AA with the slits set at 50 \AA and a wavelength reproducibility of 0.1 \AA . The optical signal was detected by HamamatsuR1387 photomultiplier tube with an S20 response, sent to an EG&G Model 5210 lock-in amplifier and recorded in a computer.

3 RESULTS AND DISCUSSION

3.1 Structural Characterization

The X-ray diffraction patterns of the as-synthesized Y_2O_3 sample is shown in Fig. 1(a). The diffraction peaks observed in the XRD-pattern can be indexed to cubic phase Y_2O_3 (JCPDF: 25/1200); no other phase was detected. The observed diffraction peaks correspond to the Bragg diffraction from the (211), (222), (400), (411), (332), (431), (440), (532), (622), and (613) planes. The room temperature lattice parameter of the unit cell of the yttria cubic phase estimated by the XRD patterns was 10.6051 \AA which was in good agreement with the JCPDS database of pdf number 83-0927.



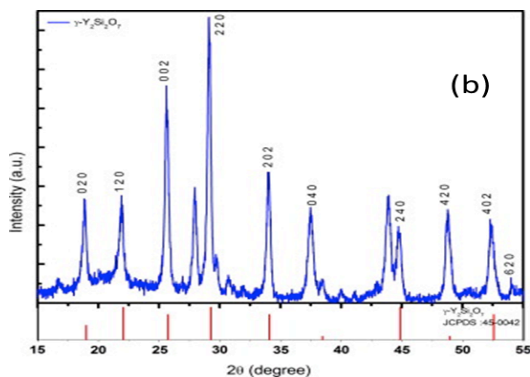


Figure 1: XRD pattern of the as-synthesized Y_2O_3 (a) and γ - $Y_2Si_2O_7$ (b) nanocrystalline powders.

Fig. 1(b) shows the XRD pattern of the nanoparticles synthesized by the sol-gel method annealed at 1170 °C for 12 h. The monoclinic γ - $Y_2Si_2O_7$ phase with the P21/c space group of the powder were matched by comparing the peak positions and intensities with those in the joint commutation powder diffraction standards (JCPDS). It can be clearly seen from the figure that the positions of most of the diffraction peaks of powder correspond well to the JCPDS card of γ - $Y_2Si_2O_7$ (PDF#45-0042).

3.2 Spektroskopische Measurements

The production of WL was achieved by illuminating the Y_2O_3 nano-powder sample with the beam of the laser diode operating at 803.5 nm with an output power of 3 W. The spectrum of the WL obtained in our measurements and corrected for the sensitivity of the apparatus is presented in Fig. 2(a).

The generation of white light (WL) of γ - $Y_2Si_2O_7$ was observed by illuminating the nano-powder sample when pumped the 803.5 nm laser excitation with a 3.1 W power. The spectrum of the WL obtained in measurements of the powder and corrected for the sensitivity of the system is presented in Fig. 2(b). The inset in the figure corresponds to the corrected WL emission of γ - $Y_2Si_2O_7$ nanoparticles in the wavelength-range of 400–900 nm

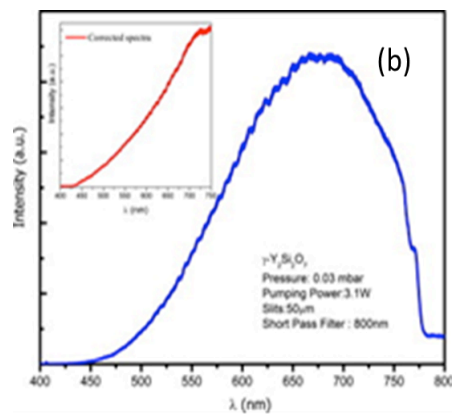
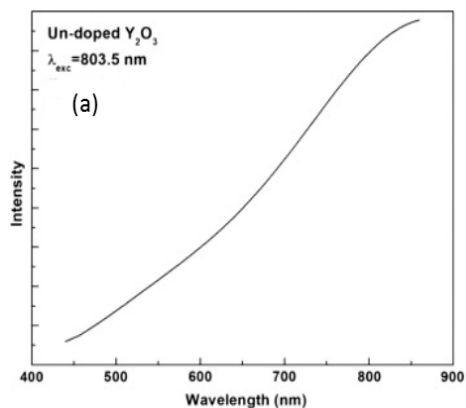


Figure 3(b) WL emission spectra of Y_2O_3 (a) and γ - $Y_2Si_2O_7$ (b) nanoparticles. The inset in the figure (b) corresponds to the corrected WL emission of γ - $Y_2Si_2O_7$ nanoparticles.

The International Commission on Illumination (CIE) coordinates and the obtained spectrum using a illuminance meter at a distance of 10 cm are presented in Fig. 4. The CIE color coordinates were found to be $x = 0.45$ and $y = 0.40$, the CCT 2756 K, and the CRI 99 for the Y_2O_3 nanoparticles.

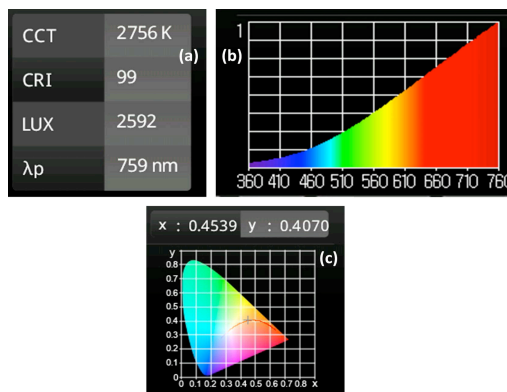


Figure 4 (a) CCT and CRI values (b) white light spectrum and (c) CIE coordinates of white light obtained by using illuminance meter.

The CIE coordinates were found to be $x = 0.3408$ and $y = 0.3100$ for the γ - $Y_2Si_2O_7$ nanoparticles under 803.5 nm excitation at 3.1W. These values lie in the yellowish region and correspond to color temperature (CCT) values of 5030 K with a color rendering index (CRI) of 85 and as shown in Figure 5.

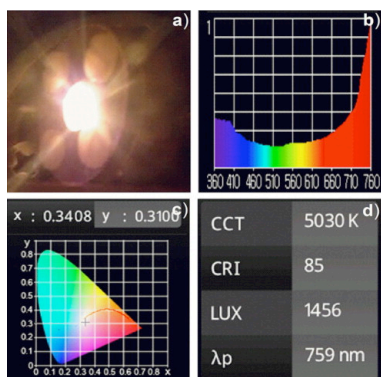


Figure 5 (a) Camera image, (b) spectral profile, (c) CIE coordinates, (d) CCT temperature, color rendering index and illuminance values of WL emission from γ - $Y_2Si_2O_7$ nano-particles.

4 CONCLUSION

When comparing the parameters of WL obtained in Y_2O_3 and γ - $Y_2Si_2O_7$ nanoparticles under the same experimental conditions it can be said that the lux value of the latter is lower than that of Y_2O_3 nanopowders.

Our findings also points out that the production of WL seems more efficient than a commercial 60 W incandescent lamp. The illuminance values for WL observed in Y_2O_3 nanoparticles and 60 W commercial incandescent lamp were measured at equal distance and found to be 2592 and 37296 lux, respectively. The former was obtained using a power of 3 W; the latter using a power of 60 W. The ratio lux/W was then 864 for the WL and 622 for the lamp, making the WL more efficient. Also the obtained CRI value (99) of our WL is equal to that of a commercial incandescent lamp. The lamps with CCTs above and under 4000 K are considered as cool and warm in appearance, respectively [12]. The lights with the CCTs under 4000 K and with high CRI (>80) are very good candidates for indoor are very good candidates for indoor lighting and are considered very close to natural light [12]. So, the CRI, CCT and illuminance values obtained by us make our WL a good candidate for indoor lighting.

REFERENCES

- [1] J. Wang, P.A. Tanner, J. Am. Chem. Soc., 132 (2010), pp. 947–949
- [2] A.K. Singh, S. Singh, D. Kumar, D.K. Rai, S.B. Rai, K. Kumar, Opt. Lett., 37 (2012), pp. 776–778
- [3] S. Redmond, S.C. Rand, X.L. Ruan, M. Kaviany J. Appl. Phys., 95 (2004), p. 4069
- [4] M.L. Debasu, D. Ananias, I. Pastoriza-Santos, L.M. Liz-Marzan, J. Rocha, L.D. Carlos, Adv. Mater., 25 (2013), pp. 4868–4874

- [5] W. Strek, L. Marciniak, A. Bednarkiewicz, A. Lukowiak, R. Wiglusz, D. Hreniak, Opt. Express, 19 (2011), p. 14083
- [6] G. Bilir, G. Ozen, J. Collins, B. Di Bartolo, Synthesis and spectroscopic properties of nano-scale $Y_2O_3:Nd^{3+}$ phosphors, ECS Trans., 50 (41) (2013), pp. 1–7
- [7] M. Erdem, G. Ozen, C. Tav, B. Di Bartolo, Ceram. Int. 39 (2013) 6029–6033
- [8] G. Bilir, G. Ozen, J. Collins, B. Di Bartolo, Appl. Phys. A, 115 (1) (2014), pp. 263–273
- [9] G. Bilir, et al., Applied Physics A, 2014. 115(1): p. 263-273.
- [10] W.Y. Ching, L. Quyang, Y.N. Xu, Phys. Rev. B 67 (2003) 245108.
- [11] G. Bilir, G. Ozen, B. Di Bartolo, Opt. Spectrosc. 118 (2015) 131–134.
- [12] M.R. Krames, O.B. Shchekin, R. March, G.O. Mueller, L. Zhou, G. Harber, M.G. Craford, J. Disp. Technol., 3 (2007), pp. 160–175